Community Earth System Model climate under Last Glacial Maximum boundary conditions

Ruth Julia Ladwig

2nd March 2021

Abstract

Results are shown from the fully coupled Community Earth System Model,(CESM), of the Last Glacial Maximum (LGM) with an orbital forcing of 22,000 BCE. This orbital forcing results in an atmospheric CO_2 concentration of 213.1ppm for the LGM. The sea surface temperature (SST) decreased by 2.30 °C globally and 2.05°C at the tropics, both well within proxy reconstructions (Brady et al. 2013). Increase ice extent causes a strengthening of sea surface windstress leading to a shift equatorially of the westerlies in the Southern Ocean (SO) and in the North Atlantic and Pacific Oceans. The Atlantic meridional overturning circulation (AMOC) strengthens in with glacial forcing along with a shoaling of the North Atlantic deep water and a filling of the deep basin up to sill depth with Antarctic bottom water. The increased AMOC strength increases the strength of the North Atlantic sub-polar gyre, transporting warm salty water further north into the Labrador Sea and deepening the maximum boundary layer along the ice edge. The increased strength of the AMOC has led to a weakened cooling in the Northern Hemisphere, 0.736°C, compared to the Southern Hemispheres cooling of 1.52°C. The transport through the Drake Passage increase with the strengthening of the SO westerlies and an increased AMOC strength. The CESM was also compared the CCSM4 output for LGM and PI simulation. The CESM and CCSM4 had similar sensitivity for glacial forcing for ice cover, SST change and windstress. The AMOC in the CESM was less sensitive to glacial forcing the the CCSM4.

Contents

1 Introduction **3**

2 Scientific Background **3**
2.1 Paleoclimatology 3
2.2 The Last Glacial 5
2.3 Atlantic Meridional overturning circulation 6

3 Experimental Setup **8**
3.1 Model Description 8
3.2 Model Setup 9

4 Results **10**
4.1 Temperature and Salinity 10
4.2 Spatial response of Sea ice 11
4.3 Sea Surface Wind-stress 13
4.4 Ocean transports 14
4.5 Boundary Layer 15

5 Discussion **17**

6 Model comparison **20**

7 Conclusion **22**

1 Introduction

The complex interplay of the ocean, ice and atmosphere and its role on the climate still remain unsolved. Evidence from proxy records alongside climate models have allowed us to understand what we do know about the climate so far. Proxy have allowed us to investigate past climate. Evidence from lake and ocean sediment and ice cores have shown a cycle that dates back by approximately 500kyrs called the glacial inter-glacial cycle. This cycle shows variations in atmospheric concentration of CO_2, temperature and ice volume. These variations have an intertwined relationship with other components of the climate; sea surface windstress, AMOC and maximum mixing layer. What drives this cycle and how this affects other components of the climate is still not fully understood. Although there have been many contesting theories attempting to explain them.

Numerical models play a crucial role in our understanding of the climate system. Without models it is not possible to test hypothesis in how the climate reacts to different changes globally or locally. Due to this, models need to be regularly evaluated and improved. All model errors need to be analysed and corrected. Traditionally past climates have been done with lower-resolution versions by modelling groups or different versions of the model. Using the same model for past and future climate change experiments enhances the progress in understanding the climate and its components.

The Last Glacial Maximum (LGM) has been investigated in detail as it is thought to provide a good test for climate model response to insolation and green-house gas driven changes. Much is known about the climate during the LGM from proxy records, although the climate has not been completely evaluated. We use the pre-industrial climate for comparison when evaluating models as it has be proven to be a reliable control.

In this thesis The Community Earth System Model (CESM) a fully coupled model, with active biochemistry where a contribution of mixing and insolation changes drives the climate is investigated. These simulations consist of a 1000 year spin up with pre-industrial (PI) insolation and two 3000 year perturbation period of insolation. One driven by PI insolation and the other driven by the LGM insolation. Just by accounting for orbital forcing and replacing today's bathymetry and ice sheet orography with the one described in Peltier et al. (2015) there was a decrease of approximately 55 ppm of atmospheric carbon dioxide. In this thesis we will compare sea surface temperature changes between the LGM and PI with the Multi-proxy Approach for the Reconstructions of the Glacial Ocean Surface(MARGO) reconstructions averaged globally, over the tropics and the northern and Southern Hemisphere from Brady et al. 2013.

2 Scientific Background

2.1 Paleoclimatology

Climate variables such as temperature and precipitation require careful measurements to correctly quantify. For this reason modern climate keeping records started in 1880, when more accurate instrumentation and techniques had been developed. In order to investigate pre-1880 climates the climate community

turns to climate proxies. Climate proxies are preserved physical, chemical and biological parameters of the past that reflect the changes and characteristic of past climate where the proxy character grew or existed.

Biological proxies include trees, corals, plankton and other organisms. Their growth and/or population dynamics alter in response to a changing climate. These changes can be seen in fossils, ocean and lake sediment and tree rings. Pollen and plankton sediment, ocean and lake sediment can be used to derive quantitative estimates of past climate via statistical methods calibrated against modern distribution parameters(Sorooahian and Martinson 1995). The chemistry of several biological and physical proxies reflects well-understood thermodynamic processes. These can be transformed to estimate climate parameters. These include oxygen isotopes in coral and foraminiferal carbonate which infers past temperature and salinity; magnesium/calcium and strontium/calcium in carbonate which infers about past temperature, oxygen and hydrogen isotopes, and combined nitrogen and argon isotopes in ice cores (Jansen et al. 2007).

Rayleigh fractionation is exponential relation that describes the partitioning of isotopes between two reservoirs as one reservoir decreases in size. It allows us to analysis changes in isotopes in ice cores, ocean and lake sediments. For example, oxygen isotopes in water; the heavier isotope, ^{18}O precipitates and condenses at higher temperatures then the lighter isotope ^{16}O . Consequently, the precipitation at high latitudes contains more ^{16}O. If the relative abundance of ^{18}O increases at higher latitudes we can surmise there has been a global increase in temperature, a warm period(Jouzel, R.D.Koster and Russell 1994).We can identify the temperature variation from the ratio of ^{18}O and ^{16}O in ice cores taken from Antarctica and Greenland. The isotopic ratio is often expressed in δ-notation using the equation:

$$\delta(in‰) = (R_x/R_s - 1) \cdot 1000$$

where R_x is the ratio between the heavy to light isotope and R_s donates a reference of a standard ratio (Kendall, McDonnell and Caldwell 1998).

Ageing proxies is an important part of paleoclimatology as knowing when the climate fluctuations happened is important for how they relate to not only other proxies but also changes in insolation due to orbital forcing. This allows us to paint a better picture of how all the climate components interact. Dating records are done through proxies that have annual layers such as corals, sediment ice cores and some cave deposits. As well as through radiocarbon chronology. Multiple sources are normally used in order to reduce age uncertainty.

The field of paleoclimatology depends heavily on replication and cross verification between paleoclimate records from independent sources in order to build confidence in inference and past climate variability. Proxy reconstructions and paleo-data has it limits as it does not allow us to infer what the cause and effect of changing climates are. For example, ice core records show a great link between local temperature in Antarctica and the globally mixed gases, CO_2 and methane, but casual connections between these variables are best explored with help of models. Developing a quantitative understanding of the mechanisms that caused these changes is the most effective way to learn about and from proxy data and climates.

Models are important to testing physical hypothesis quantitatively. Models allows the linkage between cause and effect in past climates and past climate

change. It is important that the same climate model can simulate both present, future and past climates using differences in prescribed forcings. Though it is preferable that long simulations are usually required to model past climates and computing power is a limiting factor, faster coupled models are often used. Coupled climate models perform generally better than atmosphere-only models, revealing the amplifying roles of ocean and land surface feedbacks in the climate. Additional components are commonly added in paleoclimate applications that are used in simulations of modern climate such as components that track the stable isotopes. Vegetation modules are included in order to both capture the biophysical and biogeochemical feedback as well as to validate models against proxy data.

2.2 The Last Glacial

Paleoclimate records document that Earth's ice cover has increased and decreased several times in the past. When the ice sheets are large, we call it a glacial period and when they shrink; the inter-glacial period. The cycle between these two is called the glacial-interglacial cycle. The glacial–interglacial cycles are apparent in ice core for the 740 Kyrs and several million years in oceanic sediments. In the Holocene and mid-Pleistocene the glacial and inter-glacial periods occurred in a cycle of 95 to 120kyrs which correlates with the Milankovitch cycles(Hays, Imbrie and Shackleton 1976). The Milankovitch cycles are the variations of the three dominant orbital parameters; eccentricity, obliquity and precession that cause a variation in insolation(Milankovitch 1941). The change in insolation effected the temperature, ice volume and atmospheric carbon dioxide. These changes to the climate cause feedback loops. The relationship between temperature, ice cover and carbon dioxide is a positive feedback. A positive feedback is one that the effect of a small perturbation cause an amplification of that perturbation. An example of a positive feedback is the ice-albedo feedback. This is when there is a decrease in temperature leading to an increase in ice and snow cover resulting in an increase in albedo which then leads to a decrease in temperature.

The 100 kyr cycle is made up of a slow glacial build up period of ≈ 90 kyrs. When this reaches its maximum we call it the glacial maximum. Which is then followed by a short inter-glacial period of ≈ 10 kyrs, where the ice sheets melt and reduce in size. The deglaciation happens much faster than the glaciation due to the positive feedbacks having a much stronger effect. There are two dominant feedback systems. One is the ice-albedo feedback. A second feedback involves atmospheric carbon dioxide. Direct measurement of past CO_2 trapped in ice core bubbles shows that the amount of atmospheric CO_2 decreased during glacial periods. In part because the deep ocean stored more CO_2 due to changes in either ocean mixing or biological activity. It also reduced due to more CO_2 being trapped in ice bubble. Lower CO_2 levels weakened the atmosphere's greenhouse effect and helped to maintain lower temperatures. Warming at the end of the glacial periods liberated CO_2 from the ocean, which strengthened the atmosphere's greenhouse effect and consequently contributed to further warming. Compilations of terrestrial and surface ocean climate reconstruction indicate a coherent picture of cooler and drier conditions globally, consistent with the records of terrestrial biome distributions. Whilst the greenhouse effect is thought to be the dominant driver of temperature change at low latitudes, where cooling

was of the order of 2–3 °C. The effects of the ice sheets were largest over North American and Eurasian land areas, where annual mean cooling was of a much greater magnitude and with larger seasonality Jansen et al. 2007. Using proxy records it has been found that the last glacial cycle occurred between 110.8 kyrs before present (BP) and 11.7 kyrs (Hughes, Gibbard and Ehlers 2013) with the last glacial maximum occurring at 26.5 kyrs to 19 kyrs BP(Clark et al. 2009).

2.3 Atlantic Meridional overturning circulation

The Ocean circulates due to a combination or mechanical and density forcing; Wind stress, tides and variations in surface density. The surface density is altered through exchanges of heat and freshwater with the atmosphere through evaporation and in the polar latitudes, sea ice melting and freezing. Whenever the surface water becomes denser than the deeper water, convection occurs. The density contrast leads to horizontal pressure gradients. Dense water formed at high latitudes can sink to great depths and spread horizontally. It is replaced by the lighter less dense water creating an overturning circulation.

The AMOC (Atlantic meridional overturning circulation) dominates the ocean's heat transport directed northwards at all latitudes and a southward flow of colder, deep waters that are part of the thermocline circulation. The AMOC transports warm, salty (spicy) surface water from the tropics northward with the gulf stream. When it reaches Greenland and Iceland it sinks into the deep ocean due to the freshwater output from melting sea ice. The water that sinks and is formed in the North Atlantic is called North Atlantic deep water (NADW). This water then flows southward at a depth of about 2–3 km and eventually rises back up to the surface in the Southern Ocean (SO).

Regions of upwelling are where a divergence of surface waters causes Ekman suction and an upward flux of deep water. The net northward heat transport in the Atlantic is unique among global oceans and is responsible for the relative warmth of the Northern Hemisphere (Buckley and Marshall 2016). AMOC carries up to 25% of the northward global atmosphere-ocean heat transport in the Northern Hemisphere. As well as acting as a heat pump and high-latitude heat sink, AMOC is the largest carbon sink in the Northern Hemisphere, sequestering approximately 7 10^{14} g of carbon per year (Gruber, Keeling and Bates 2002).

There are 4 main regions of overturning; convection and return flow in the Nordic Sea, convection and entrainment in the Labrador Sea, the equatorial and coastal Atlantic upwelling and the SO upwelling. The NADW is primarily upwelled in the SO. This is also the primary up welling associated with the AMOC on a Global scale 80% of upwelling happens in the SO (Talley 2013). The upwelling supplies large amount of nutrient from the deep ocean to the sea surface. After upwelling the water goes one of two paths. The water that upwells more south near to the sea ice forms dense bottom water. Water that upwells at lower latitudes moves northward due to Ekman transport. Due to the conservation of mass the ocean must downwell an equal volume of water as is upwelled. Upwelling in the Atlantic Ocean itself occurs at the equator and coastlines. Coastal upwelling occurs due to Ekman transport along the interface between land and wind-driven current. The upwelling at the equator occurs due to atmospheric forcing and divergence due to the opposing direction of the Coriolis force either side of the equator.

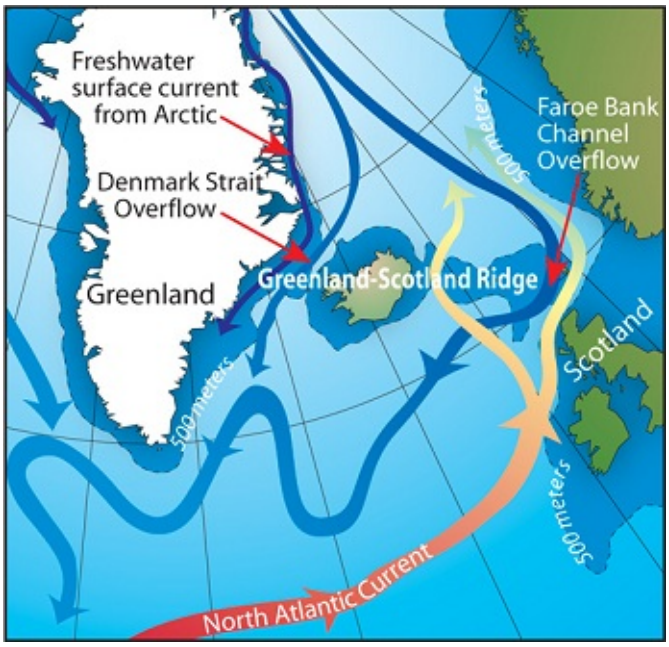

Figure 1: Nordic Sea Overflows Locations and directions.(Oberlander n.d.)

At the Nordic Sea, due to the high latitude, the temperatures are lower. These lower temperatures drive a density increase and convection in the water column. In the open-ocean convection spreads into deep plumes. The temperature difference between sea and air is much larger in winter making the convection stronger. The Nordic Seas Overflow Water (NSOW) is made of several overflows. Most of the dense water flow flows towards the Denmark strait forming the Denmark Strait Overflowing Water (DSOW). The other two overflows in the Nordic Sea are through the Iceland-Faroe ridge and through the Faroe-Shetland Channel these two flows make up the Iceland Scotland Overflow Water (ISOW). These overflows can be seen in figure 1. As ISOW overflows the Greenland Scotland ridge it turbulently entrains intermediate density water, sub-polar and Labrador Sea water LSW. This grouping of water-masses then moves geostrophically southward along the East flank of Reykjanes Ridge, through the Charlie Gibbs Fracture Zone and then northward to join DSOW. NSOW flows cyclonically around the Labrador Sea and further entrains LSW. Convection is known to be suppressed at these high latitudes by sea-ice cover. Floating sea ice "caps" the surface, reducing the ability for heat to move from the sea to the air. This in turn reduces convection and deep return flow from the region.

The Labrador Sea is an arm of the North Atlantic between the Labrador peninsular and Greenland. The Fresh LSW is formed at intermediate depths by deep convection in the central Labrador Sea. This convection is not deep enough to penetrate the NSOW layer which forms the deep waters of the Labrador Sea. LSW joins NSOW to move southward out of the Labrador Sea. The LSW production is highly dependent on sea-air heat flux and yearly production is approximately 3–9 Sv (Zantopp et al. 2017). An increase in LSW production is

associated with an increase of strength of the North Atlantic sub-polar gyre.

The AMOC is vulnerable to climate changes as density is its main driver. Paleoclimate reconstructions suggest not only was the glacial AMOC is different from today in key aspects such as vertical extent, but it may have declined significantly at times in the past 20Ka in response to large melting water events associated with deglacial warming and sea level rise. A reduction in AMOC strength suggests reduction in northward ocean heat transport. This cools the NH and warms the SH; these are noted as Dansgaard-Oeschger (DO) events. This redistributes heat through the bipolar seesaw which does not affect the global mean. Several fluctuations of the AMOC have happened in the past. This can be seen in Greenland proxy (Stocker and Johnsen 2003a). The amplitudes of these rapid warmings in Greenland have been estimated using the changes in the stable isotopes of enclosed air to range from 9°C up to 16°C(Lang et al. 1999). It has been suggested that changes in the strength of the AMOC could have an effect on global temperature and atmospheric CO_2 concentration. It has been suggested that a collapse of the AMOC due to an increase of freshwater forcing could cause and increase of CO_2 out gassing in the SO.

Many studies have been done, into what causes fluctuations in the AMOC strength by testing its sensitivity to various forcings such as SO winds, freshwater forcing, temperature and ice cover. The relationship between SO winds and the AMOC strength has been investigated several times with various models. Studies have been done of AMOC's sensitivity to glacial forcing with varying results. Model simulations have shown varying results for the glacial Atlantic Ocean. The PMIP2 simulations showed differing AMOC responses to glacial forcing, whereas the latest PMIP3 simulations found a stronger and deeper AMOC. As well the radiogenic isotope ratio of protactinium-231 and thorium-230, that can be used to reconstruct flow rates, reconstructions are inconclusive about the strength of the AMOC during the LGM (Breitkreuz, Paul and Schulz 2019). The depth and strength of AMOC are shown to be strongly correlated with the depth of heat storage across a suite of general circulation models (GCMs). Models with a deeper and stronger overturning circulation, store more heat at intermediate depths, which delays the surface temperature response on multidecadal time scales.

3 Experimental Setup

3.1 Model Description

The tool used in this thesis is the coarse resolution version of fully coupled (atmosphere-ocean-land-sea ice) Climate Earth System Model 1.2 (CESM). The model is spun for 1000 years using 1850 CE (pre-industrial, PI) orbital forcing. After the first 1000 years the simulation split into two, the PI and the LGM. The PI is run for another 3000 years with no perturbation and is used as the control. The LGM is run for another 3000 years with the orbital forcing 22,000 years before common era (BCE). The LGM represents the planet at the Last Glacial maximum. The result used for analysis is the average of the last 100 years of each run. The difference LGM-PI is used to investigate how the perturbation influences the variables within the model.

3.2 Model Setup

The model setup is based on Nielsen et al. 2019, where a more detailed description of the parameterisation can be found. The ocean model is run with the Dent and McWilliams 1990 parameterisation using a stratification dependent thickness and isopycnic diffusivity. The ocean resolution caries with latitude from 400 km near the equator to 20 km at the poles. The resolution also varies with longitude from 400 km to 40 km in the meridian resolution with the largest values in the North Pacific. The ocean resolution also varies with depth. There are 60 vertical layers of non-uniform thickness, ranging from 10, at the surface to 500m at the bottom. The atmospheric model uses a T31 spectatorial truncation in the horizontal with 26 vertical layers. The biochemistry is coupled to the climate system and exchanged carbon between ocean land and atmosphere.

Historically the process of breaking internal waves in the ocean has been represented as constant diffusivity. This process converts turbulent kinetic energy to potential energy and is hypothesised to cause the AMOC collapse. The internal mixing from these waves has an effect on the biogeochemistry of the ocean. This means that the constant parameterisation of internal waves cause a loss of information. Therefore, as proposed in Nielsen et al we use the vertical mixing parameterisation, IDEMIX, where the internal wave energy and dissipation rate are calculated for each grid cell in the sea. In Nielsen et al 2019 a perturbation of the insulation is made from PI to 113,000 BCE this cause the AMOC strength at 26 degrees north to decrease from 12Sv to below 5 Sv during the first two centuries. This is due to the increased sea ice export from the Nordic Sea to the North Atlantic increasing the surface stratification and inhibiting deep water formation(Jochum et al. 2010). Showing that the IDEMIX is free of any assumptions regarding localisation and strength of the applied freshwater forcing.

4 Results

	PI Control	LGM
Global pCO_2(ppmv)	268.2	213.1
Global sea surface T(°C)	6.801	4.498
Tropical sea surface T (°C)	24.95	22.90
Southern Sea Surface T (°C)	7.292	5.772
Northern Sea surface T(°C)	0.672	-0.164
AMOC (Sv)		
NH max	13.46	20.19
Max at 34°S	11.00	13.52
Sea ice are ($10^6 km^2$)		
NH	16.11	13.65
SH	16.11	26.50

Table 1: Summary of climate changes of PI and LGM. Annual means are computed over the last 100 years. The southern sea surface T is the average Sea surface temperature bellow 30 degrees south and the northern aea surface temperature is the average temperature above 30 degrees north. The Global sea surface temperature and Global pCO_2 are average over the whole Globe.

4.1 Temperature and Salinity

The global average sea surface temperature (SST) decreases by 2.303 °C from the PI control to the LGM (Table 1). There is a large decrease in SST at the Norwegian Sea along the the ice edge. The sea surface temperature has decreased for both the southern and Northern Hemisphere. The Southern Hemisphere sea surface temperature decreases by 1.520 °C. The decrease in the Northern Hemisphere is 0.836 °C which 40% less the in the Southern Hemisphere. (Figure 2 Figure 13). Figure 3 shows the zonally averaged temperature in the Atlantic Ocean for the Pi and LGM case as well as the change in temperature LGM-PI. There is cooling all through the depth of the Atlantic Ocean except for a small increase of temperature at the surface of the Antarctic Sea. The Largest Change in temperature of -6°C is in the North Atlantic at about 40° north and 1km depth.

Figure 4 shows the ocean stratification for the Atlantic basin and the Pacific basin. The stratification in the Pacific basin is mostly unchanged between the LGM and PI cases with an exception of increase of stratification between 3 and 5 km depth in the LGM case. The stratification in the Atlantic Ocean decreases between 2km and 3km for the LGM case compared to the PI case. The stratification almost halves in the LGM case for the Atlantic Ocean.

Figure 6 shows the zonally averaged salinity difference (LGM-PI) of the Atlantic Ocean. Figure 5 shows the change is sea surface salinity LGM-PI. Although most of the sea surface does not have as large of a change in salinity. There is an increase in surface salinity where there has been an increase in ice cover the largest increase being in the Labrador Sea. There is also a large

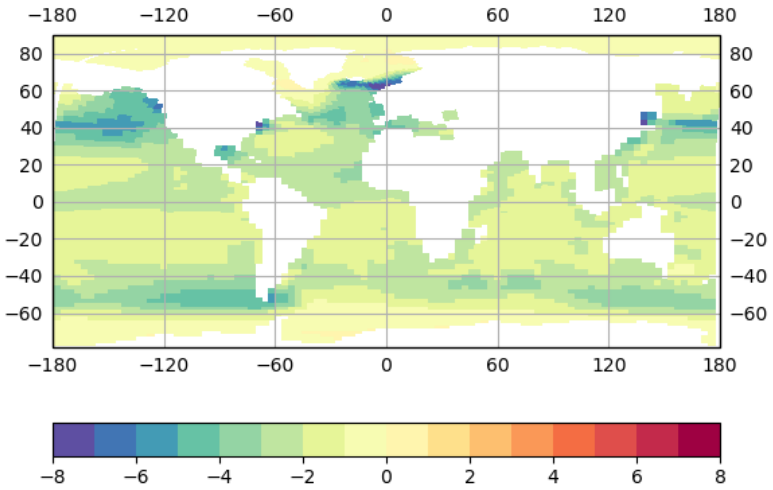

Figure 2: Sea surface temperature difference between LGM and PI.

decrease in salinity at the Florida Strait. The Pacific and Indian Ocean surface salinity is almost unchanged.

Figure 7 show the Sea surface temperature at the tropics for the PI, LGM and the difference between the two (LGM-PI). There is a decrease in temperature across the whole tropics with the largest decrease being off. the west coast of Africa and at the Florida strait in the LGM compared to the PI case.

4.2 Spatial response of Sea ice

There is a large increase, in annual mean sea ice area in the Southern Hemisphere of 65% from PI to LGM with a further extent equatorial (Table 1,Figure 9). The Northern Hemisphere sea ice change is not so easily evaluated due to the expansion of land, meaning the Arctic ocean has decreased in size. There is a decrease in sea ice area in the Northern Hemisphere from PI to LGM of 15% (Table 1). Alternatively seen in Figure 8 there is an increase in average annual ice cover in the lower latitudes with the ice extent reaching further out. This can be seen at the Pacific sub-polar region and the Barents Sea. Also in the Labrador Sea, the sea ice has expanded further into the North Atlantic with a much higher sea ice fraction. Except for an area of reduction of sea ice fraction off the west coast of Greenland in the Labrador Sea.

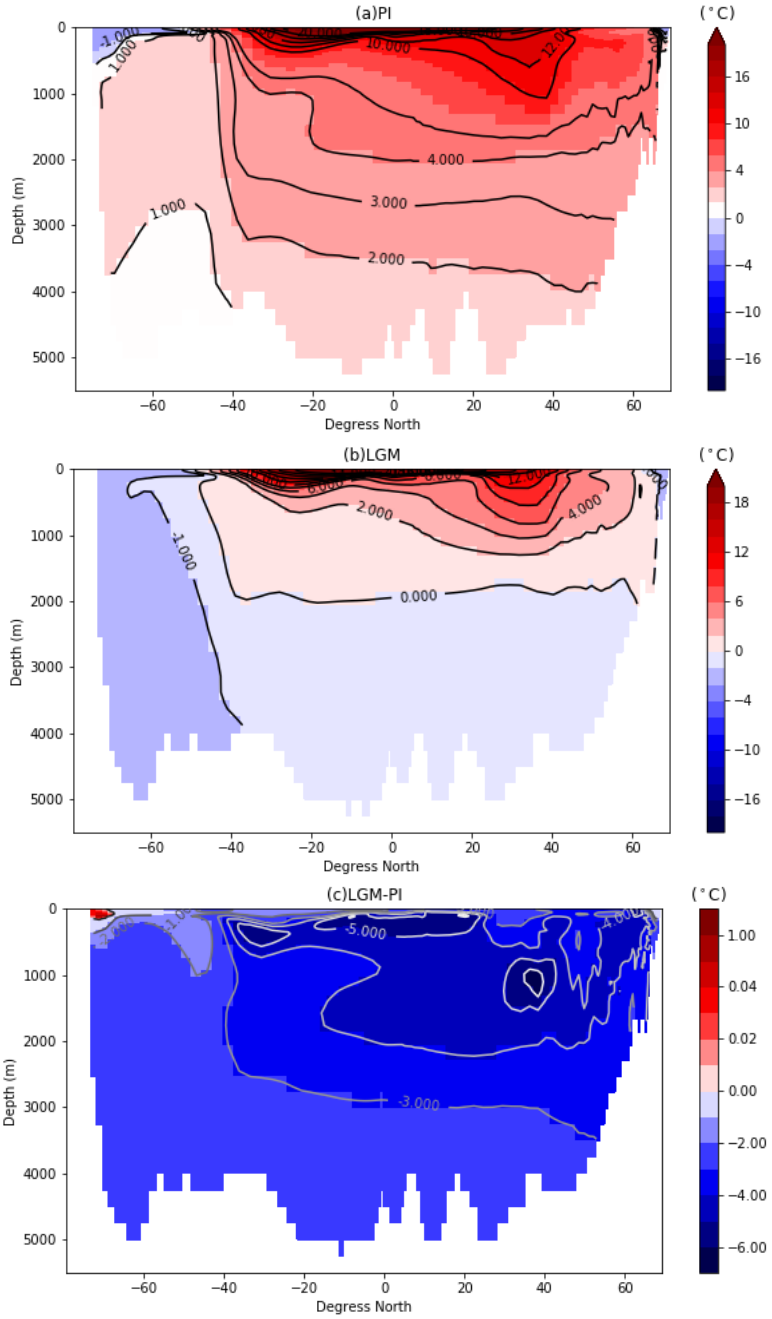

Figure 3: Zonally averaged temperature in the Atlantic Ocean (a) is for the PI case (b) for the LGM case and (c) is the difference between the LGM and PI. Contour lines represent 1°C

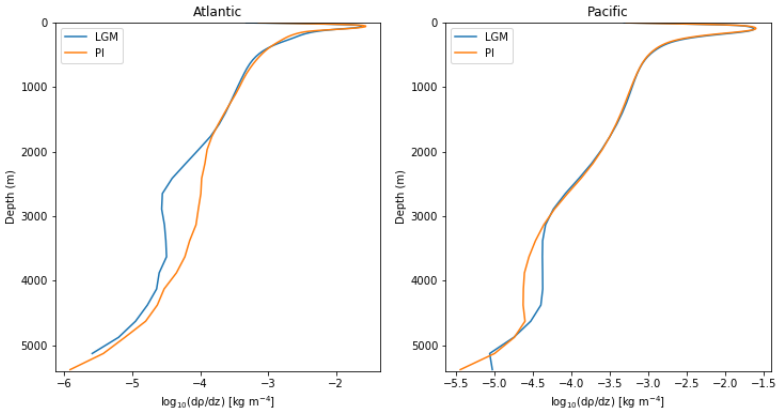

Figure 4: Ocean stratification averaged over the Atlantic basin for(Left)and the Pacific basin (right for the LGM(blue) and PI(Orange)).

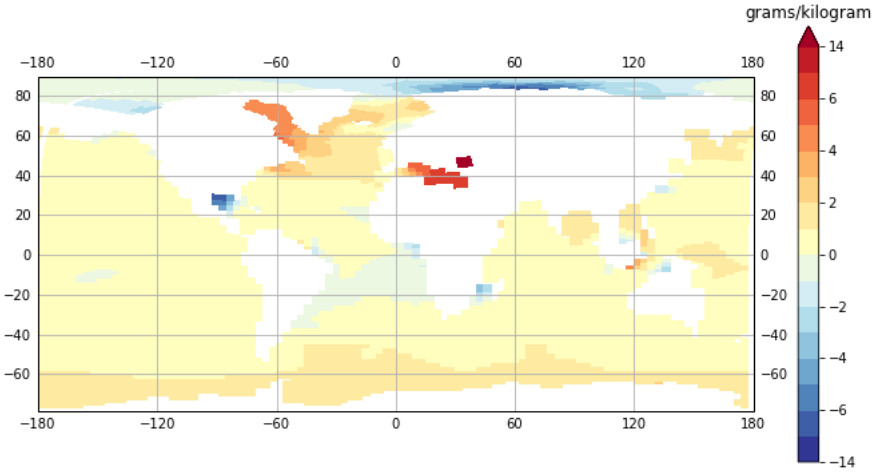

Figure 5: Sea surface salinity difference between LGM and PI.

4.3 Sea Surface Wind-stress

The Northern Hemispheres tropics easterlies increase in strengthen with the greatest response occurring in the Atlantic basin. In the Southern Hemisphere the southeasterly trade winds strengthen with the largest increase in the pacific basin and off the coast of Australia. The Southern Hemisphere westerlies have shifted further north and have increased in strength. The strengthening is at its greatest just equatorward of the sea ice edge (denoted by 50% ice fraction). In general there is a latitudinal shift of the westerlies equatorward, most likely due to the increased ice cover and the ice edge reaching further equatorward.

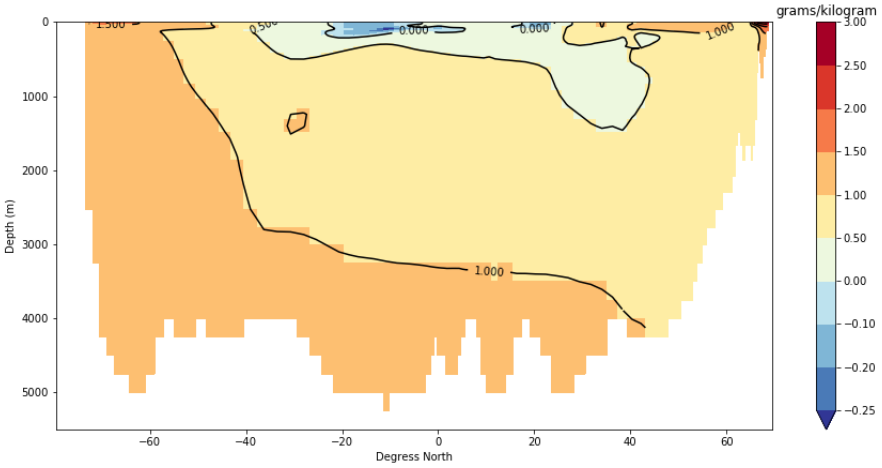

Figure 6: Zonally averaged salinity difference between LGM in the Atlantic Ocean. The contour lines represent 0.5g/Kg change of salinity concentration.

	PI Control	LGM
Wind stress (Nm^{-2})		
Max	1.402	1.502
Drake Passage	0.981	1.229
Average	0.333	0.433
ACC Drake Passage (Sv)	98.55	102.4

Table 2: List of key aspects of the ACC. With the max being the maximum of the zonally averaged zonal wind stress, Drake Passage being the wind stress at the southern tip of south America, average windstress over the whole ACC (all in Nm^{-2}). ACC Drake Passage is the barotropic transport through the Drake Passage in Sverdrops.

4.4 Ocean transports

Figure 11 compares the strength of the zonally averaged AMOC in sverdrops of the LGM and PI case. The Location of the maximum AMOC at a depth of approximately 1000m and 35 degrees north does not vary greatly between the LGM an PI case. Although the upwelling at this point is much stronger in the LGM simulation. The strength of the AMOC increase in LGM for both the maximum and at the outflow latitude.

There is a shallowing of the zero contour separating the clockwise circulation of NADW, produced from the formation and sinking in high northern latitudes, and from the counterclockwise circulation of simulated Antarctic Bottom Water (AABW) in the PI case compared to the LGM. The zero contour is at $\approx$ 2800 KM in the pi and $\approx$ 3200 KM in the LGM.

The transport through the Drake Passage is greater in the LGM case than the PI case. Table 2 show that the wind stress and the Antarctic Circumpolar circulation (ACC) through the Drake Passage are greater in the LGM case.

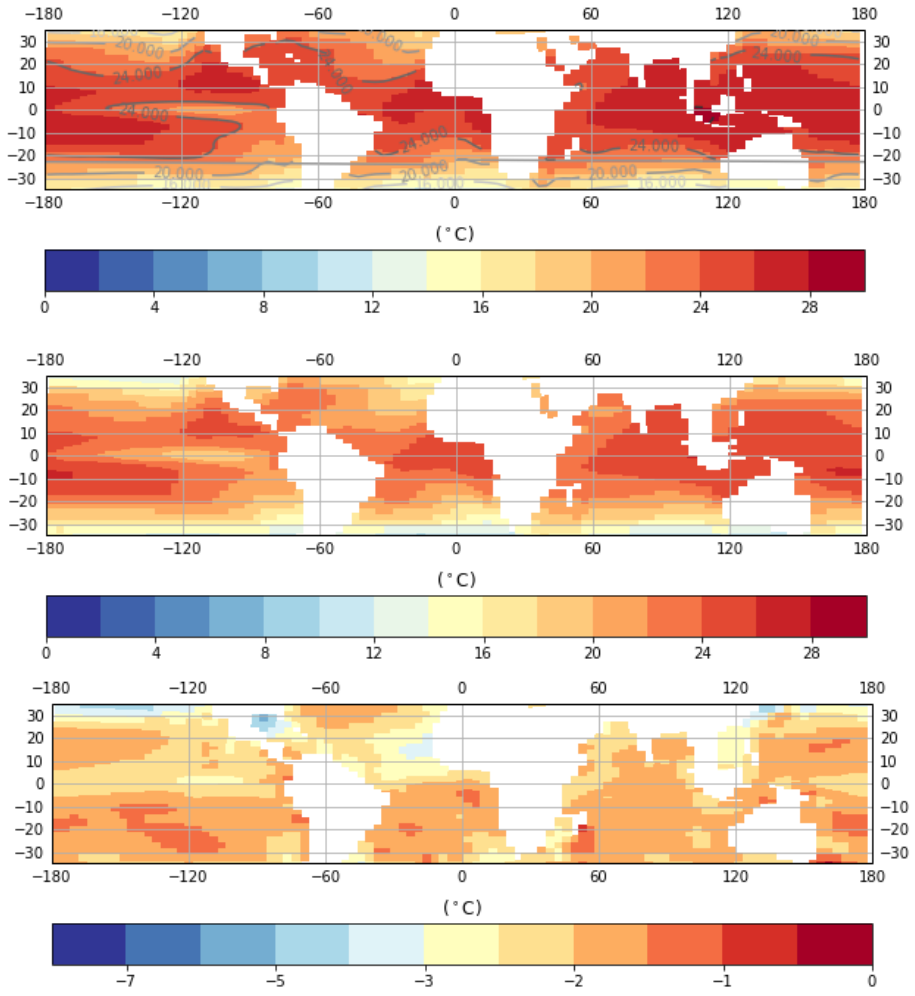

Figure 7: Annual average Tropical Sea surface temperature (a)PI (b) LGM (c)LGM-PI

An increase of 25% in the windstress through the Drake Passage has led to an increase of 4% in transport through the Drake Passage.

4.5 Boundary Layer

Figure 12 Shows the maximum boundary layer, ice fractionation and barotropic stream function for the sub-polar North Atlantic. The barotropic streamfunction shows the strength of the North Atlantic sub-polar gyre.

The boundary layer increases in depth from the PI case to the LGM case and moves equatorward along with the increased sea ice cover, (Figure 12). The decreased depth is correlated with the increased strength of the North Atlantic sub-polar gyre seen at the bottom plot in Figure 12 and with the increased strength of the AMOC.

There is also a deepening of the boundary layer on the east coast of Green-

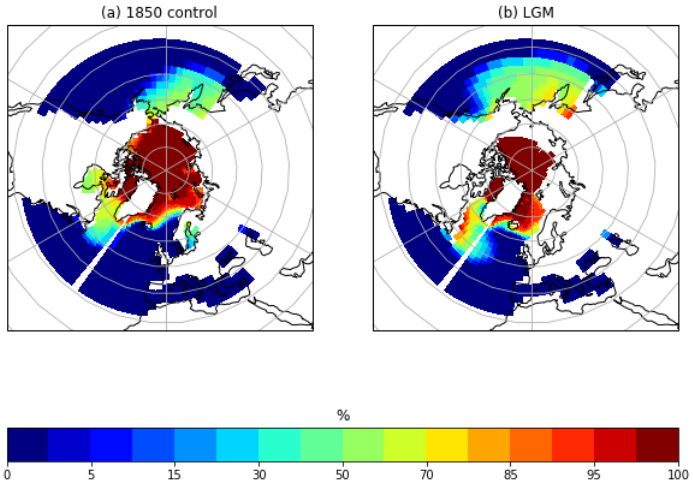

Figure 8: Northern Hemisphere Sea Ice fraction percentage.(a) PI control (b) LGM simulation.

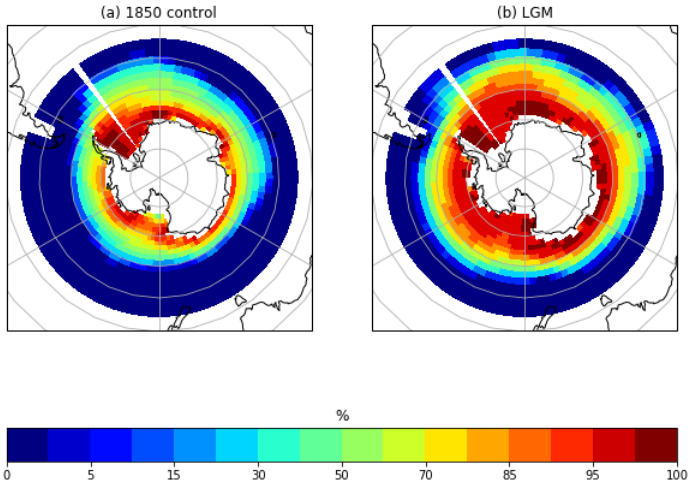

Figure 9: Southern Hemisphere Sea Ice fraction percentage.(a) PI control (b) LGM simulation.

land in the Labrador Sea for the LGM case. This will be due to the increased strength of the AMOC, causing there to be a upwelling of warmer water in the Labrador Sea. Which also causes a decrease of ice cover. This greater transport of spicy water into the Labrador Sea can be seen in Figure 5 and 13 where there is an increase in salinity and temperature in the LGM case.

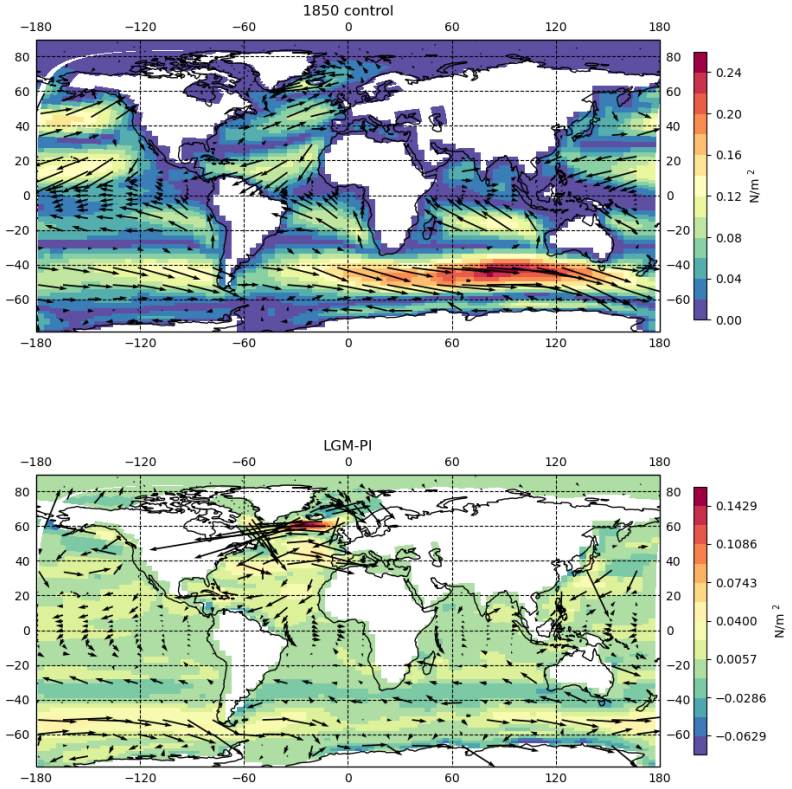

Figure 10: Map of mean annual sea surface wind stress anomalies(Nm^2)(a) is the PI situation (b) is the change in windstress

5 Discussion

The CESM when forced with the orbital forcing for the pre-industrial climate and 22,000 BCE produced a decrease in atmospheric CO_2 concentration of 55ppm. The Atmospheric CO_2 for the LGM case is 213 ppm which is higher than the proxy reconstructions $\approx$ 190 ppm (Stocker and Johnsen 2003b).This could be a result of mixing during the LGM not being fully understood or Earth system Models may indeed misrepresent one or more aspects of the various carbon pumps. As we also had an abrupt change in insolation instead of a gradual change. This gradual change of insolation can have an effect of climate interaction and the carbon pumps and mixing in the oceans allowing more carbon to be stored.

The global SST change between the PI and LGM case (-2.303 °C) is well within the latest climate proxy reconstructions of -2.1±1.8°C (Brady et al. 2013).The tropical SST -2.05°C is also with in proxy reconstruction of -1.5±1.2°C. Although it is to be noted that the grid for the proxy reconstruction is courser and is averaged over fewer points than the CESM simulation. There is also a significantly smaller increase in sea surface temperature in the Northern Hemi-

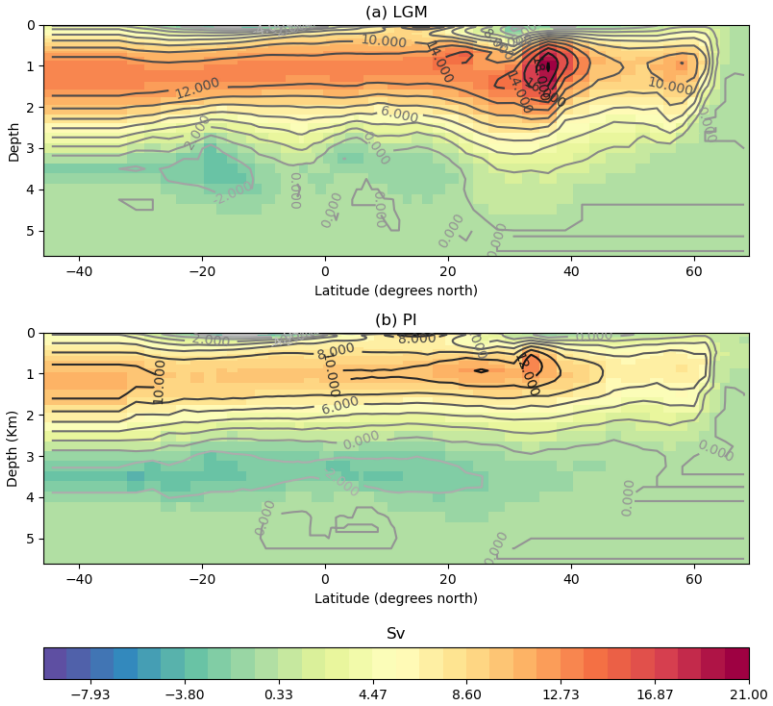

Figure 11: The mean meridional overturning circulation in the Atlantic Ocean basin for the (a) LGM and (b) PI. Positive (negative) contours are clockwise (counterclockwise) circulation. Contour interval is 2 Sv.

sphere which is due to the increased strength of the AMOC increasing heat transport to the north. This also is what causes the increase in temperature off the east coast of Greenland in the Labrador Sea. This increase in heat transport and warming also reduced sea ice in the same area.(Figure 13 and 12). The decrease in temperature and increase salinity in the deep ocean between PI and LGM is caused by an increased deep-water formation in the Ross Sea. The decrease in low depths of the Tropical Atlantic is due to the decrease in evaporation from a reduced sea surface temperature. Increase in salinity at the poles is due to Brine Rejection from increased sea ice cover.

The location of the maximum overturning in the Atlantic shows insensitivity to glacial forcing. At the latitude of the AMOC maximum there is a tight re-circulation this is a result of the strong coastal upwelling. The maximum strength of the AMOC during the PI (13.46 Sv) is not much larger than that of observations for the PI era of (12.7 Sv). The strength of the AMOC is stronger in the LGM case compared to the PI. It is difficult to evaluate whether the CESM simulated the LGM mixing accurately as several proxy reconstructions have found the AMOC weakened during the LGM and others found that it strengthened.

A strengthening of the AMOC can explain the stronger northern sub-polar gyre transporting warm water north in the Labrador Sea. This has caused the reduction of sea ice cover and the deepening boundary layer on the west coast of Greenland. There is also a deepening of the maximum boundary layer in the

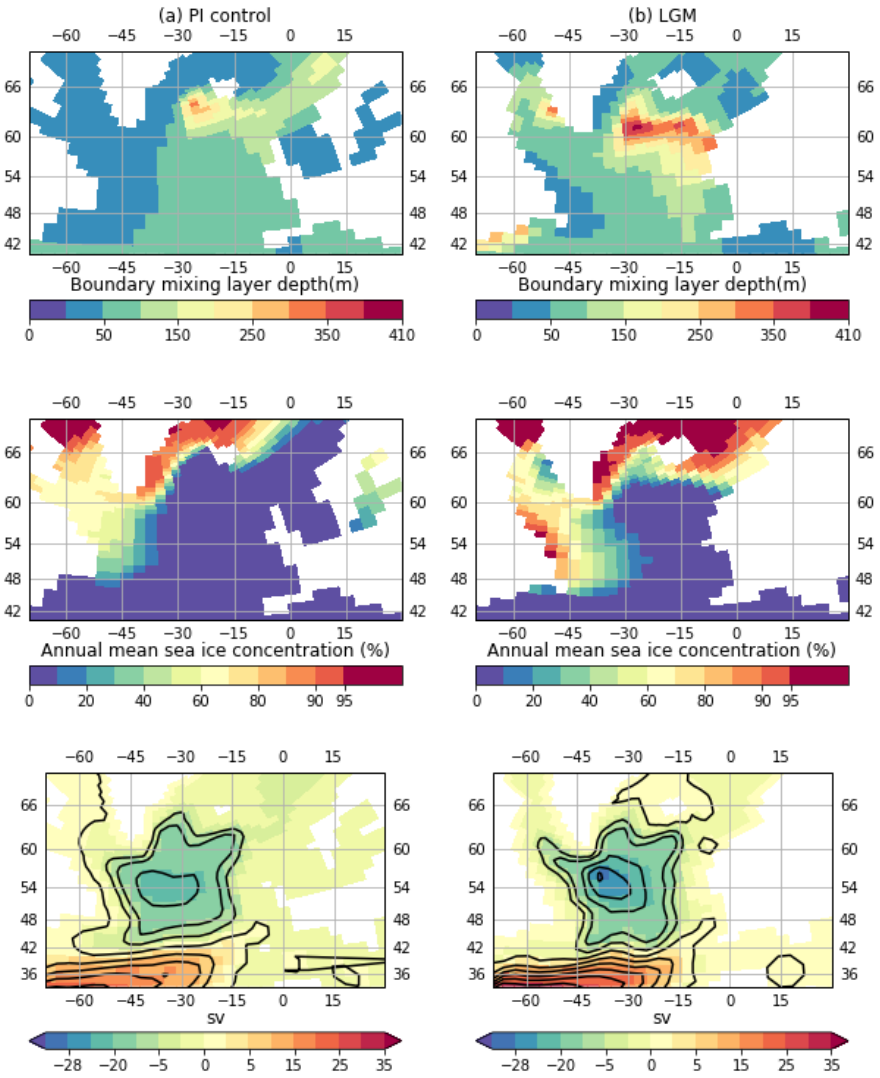

Figure 12: mean maximum annual boundary layer depth(m, top), annual sea ice concentration (%, middle)and the barotropic stream-function (sv, bottom) at the subtropical North Atlantic for (a) PI control and (b) LGM.

North Atlantic between Greenland and Norway. the maximum boundary has also moved southward due to the increase in ice sheet expansion in the LGM. The sea surface water is significantly colder along the ice edge due to the heat sink.

The AMOC is more sensitive to the adjacent boundary upwelling, of 35 degrees north as it has a much larger difference between the maximum overturning circulation and the transport at the outflow latitude 34 degrees south. This is largely caused by the southward displacement and strengthening of the North Atlantic westerlies. The AMOC strengthening could also be in part due to the increased wind stress in the SO ocean. A doubling of SO winds has been shown

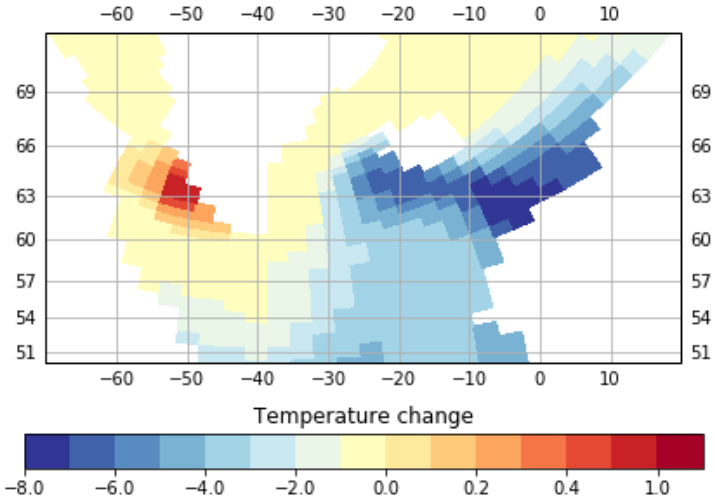

Figure 13: Difference in temperature between PI and Control in the north sub-polar Atlantic Ocean.

to increase in AMOC strength of 30% to 50% depending on the resolution (Menary et al. 2013). In this case, for an increase of 30% of average SO wind stress (Table 2) there was an increase of 18% of AMOC transport into the ACC.

The North Atlantic westerlies and easterlies increase in strength and move equatorward with the ice expansion. The strong increase in the North Atlantic along the ice edge corresponds with a deeper boundary mixing layer, and a strong sub-polar gyre in the North Atlantic. An increase in the SO windstress leads to an increase of transport through the Drake Passage. The SO ocean upwelling is wind drive. The transport through the Drake Passage appears to be sensitive to glacial orbital forcing along with SO winds. There is an increase of 4% though the Drake Passage along with a 25% increase of SO winds which goes to show there is there is low eddy saturation in this model, as the increase winds does lead to an increase in zonal transport. Though this increase of ACC transport may also due in part to the increase strength of the AMOC.

6 Model comparison

There are considerable differences between CESM and the Community Climate System Model 4 (CCSM4). The main two difference being the addition of 2 extra configurations in the CESM. A coupled ocean-sea ice model forced with atmospheric surface boundary conditions and a fully coupled atmospheric-ocean-land-sea ice coupled to a biochemistry/ecosystem/circulation modal and prognostic equations for atmospheric carbon dioxide concentration and carbon fluxes (Nielsen et al. 2019). The CESM also has a new mixing component IDEMIX.T o comapere with the CCSM4 we'll be using the results from Brady et al.

2013. The CESM run for this thesis has an atmospheric component has a smaller horizontal resolution at 3.75° compared to the CCSM 1° in Brady et al. 2013. The CCSM4 being at a higher resolution is more expensive to run but with a higher resolution you should theoretically get a more accurate reconstruction of the climate; if all components are properly understood. It should be noted that Brady et al. 2013 uses the orbital year of 1990 C.E for the PI and the CESM PI uses 1850 C.E. Another difference between this thesis's simulations and Brady et al. 2013 is the latter is forced by estimated GHGs; CO_2, CH_4 and N_2O, from high resolution ice core proxies not just orbital forcing. The atmospheric carbon dioxide in the CCSM4 for the LGM had a concentration of 185ppm. The CCSM4 also has a higher atmospheric concentration of CO_2 for their PI case. The PI case has a 1300 year integration and the LGM a 1000 year integration.

Even with a greater atmospheric CO_2 concentration in the LGM the CESM was able to simulate a similar cooling to the the CCSM4. The tropical sea surface temperature is warmer for both the LGM and PI case in CCSM4 compared to the CESM and fits with in proxy reconstructions from MARGO. However, the change in temperature between PI and LGM of approximately 2°C. Both Models have a decrease of global, Northern Hemisphere and Southern Hemisphere SST. The global decrease is greater in the CCSM4, although both are within proxy data reconstructions. In the CCSM4 the Northern Hemisphere cools by a greater degree than the Southern Hemisphere. Whereas, in the CESM it is the other way round. It was discussed earlier that the smaller degree of cooling in the Northern Hemisphere could be due to the stronger AMOC transporting heat further north however this could alternatively be due to the CCSM4 having a stronger AMOC.

The AMOC is also significantly lower in the CESM compared to the CCSM4. The CCSM4 had a max AMOC strength of 25.7 Sv and 35.8 Sv for the PI and LGM respectively. The max strength of the AMOC at 34 °S for the CCSM4 was 18.3 Sv and 20.5 Sv for the PI and LGM case respectively. Both the maximum strength of the AMOC and the export at 34°s increase for the LGM compared to the PI in both the CESM and CCSM4. There is also shoaling of the deep North Atlantic, transport with both having insensitivity to the depth of maximum transport of the AMOC. The CCSM4 higher AMOC outflow strength is too high when looking at measurements for the PI AMOC outflow. Whereas the CESM AMOC outflow is still too high but it more closely resembles that of PI measurements. This could be due to the improved mixing and diffusivity in the CESM model.

A decrease in Northern Hemisphere sea ice area occurs in both the CCSM4 and CESM LGM simulations because of the decrease in the Arctic Ocean area from the expansion of the imposed ice sheets. The sea ice expands to a greater degree in the North Atlantic for the CESM LGM than the CCSM4. the NH sea ice cover being greater in both the LGM and PI for the CESM. Similarly, to the CESM and the CCSM4 also have an area of low ice cover off the west coast of Greenland. The SH sea ice expansion in CCSM4 with an increase of 64% has a similar sensitivity to the CESM that also has a SH sea ice expansion of 64%. This similarity of sea ice cover could be the cause for the similar decrease in temperature due to the ice albedo feedback.

The wind stress response to glacial forcing over the North Atlantic is qualitatively similar in the CESM to the CCSM4 as shown by comparison of Figure 10 and in Brady et al. 2013. The NH westerlies shift southward in the sub-polar

North Atlantic and strengthen in both simulations but by a slightly greater degree in CESM. The North Atlantic easterlies strengthen to a greater degree in both the CESM and CCSM4 and shift southward. In the Pacific basin, the NH westerlies shift southward in the CCSM4 LGM simulations compared with the respective PI simulations which is similar to the CESM but strengthen slightly which they do not in this CESM case. There is a strengthening of the wind stress through the Drake Passage in both cases due to the increased ice extent. The increase is by about the same magnitude but with the wind stress being stronger overall in the CCSM4 case.

The response of the important ocean transports to LGM forcing in the CESM shows some similarities and differences compared with the response in the CCSM4. The CCSM4 transport through the Drake Passage is 175.5 Sv for the PI case and 231.7 Sv for the LGM case. The barotropic transport through the Drake Passage is lower in both LGM and PI simulations in the CESM case compared to the CCSM4. The CCSM4 transport through the Drake Passage is 175.5 Sv for the PI case and 231.7 Sv for the LGM case.

The CESM both the CCSM4 and CESM had an increase in strength of the transport through the Drake Passage, however; the CESM increased by just 4% and the CCSM4 increased by 32%. The CCSM4 ACC transport is more sensitive to glacial forcing than the CESM, the CCSM4 transport in the ACC be more driven by the

7 Conclusion

In this thesis the CESM's climate with LGM forcing has been analysed. The parameterisation follows that is outlined in Nielsen et al. 2019 was used. The model had a 1000 year spin up forced with PI insolation and then split into two separate runs of 3000 years, one with the orbital forcing of 1850 CE (PI) and one with the orbital forcing of 22,000 BCE (LGM). Just by accounting for the changed orbital forcing the LGM reconstructions, leads to a 55 ppm decrease in atmospheric CO2. Although this does not reach the lows shown in ice cores of Greenland and Antarctica of $\approx$ 190 ppm. This suggest that the CESM may misrepresent one or more aspects of the various carbon pumps or mixing during the LGM is not completely understood.

The LGM simulation has a global SST cooling of 2.30°C compared to PI conditions, with amplification of this cooling at high latitudes at the edges of the sea ice. A Tropical SST cooling of 2.05°C. Associated with these colder temperatures, the atmosphere is much drier with significantly less precipitable water. The LGM ocean is much colder and saltier than the PI. The increase in salinity in the LGM deep ocean is related to brine rejection associated with sea ice formation. The reduced cooling for the NH SST compared with the SH was discussed this may be due to the increased AMOC transporting heat further north as shown by the temperature increase in the Labrador Sea. Although the Northern Hemisphere SST decrease of 0.836°C is within proxy reconstructions (-3.2$\pm$2.7°C (Brady et al. 2013) it is on the lower than expected. As well the CCSM4 has a stronger AMOC then the CESM and it has a stronger SST cooling in Northern Hemisphere than the Southern Hemisphere of 4° C. There is an increase of global sea ice cover. The sea ice cover in the SH increases by 64% the same as the CCSM4 with the ice extent reaching father equatorward.

The Northern Hemisphere sea ice sheet does not increase in volume due to the decrease in size of the Arctic Ocean and the increased land extent, but the sea ice does reach further south into the Nordic and Labrador Sea as well as the north Pacific. The Position of the AMOC maximum is insensitive to orbital forcing. Although there is an increase in the strength of the AMOC between the two simulations for both the maximum transport and the transport at 34°S. Its difficult to say whether the increase in AMOC strength is realistic due to past proxy reconstructions showing both and increase and decrease of outflow during the LGM. Although the PI in the CESM outflow is about 6% higher then the recorded average for the time. This is also significantly closer then the AMOC outflow simulated for the CCSM4 which outflow was 44% higher then records. This would suggest that the AMOC simulated by the CCSM4 is too high. The increase in transport at 34 °S is a result of increased SO winds. The increased strength of the AMOC results in a deepening of the maximum boundary mixing layer in the North Atlantic and strengthening of the North Atlantic gyre transporting water further into the Labrador Sea. There is an increase in the transport through the Drake Passage due to the increase of sea surface windstress suggest there is minimal to no eddy saturation in the model. There have been some notable improvements for the CESM compared to the CCSM4. Despite the CESM being run at a lower resolution it was able to model changes in SST globally and in the tropic due to glacial forcing that follow proxy reconstructions similarly to the CCSM4. The CESM was also able to simulate a accurate sea ice cover for NH and SH.

The CESM with a lower resolution is able to simulated a good and accurate climate and in many aspects better then the CCSM4. Running model is lower resolution save costs and time so this would be preferable model to use. For this model we were able to run 3000 year integration's at a lower cost. It was also able to reduce the atmospheric CO_2 significantly with just orbital forcing and changes in ice orthography. While producing similar sea surface temperature changes as the higher resolution CCSM4 which boundary conditions for the atmospheric GHGs. It also had improvements on modeling the PI AMOC strength and the ACC transport through the drake passage.

There are still a number of outstanding uncertainties in our understand of the forcing and boundary conditions for the LGM. One of these uncertainties is the stability of the AMOC and the LGM ocean mixing. The model wasn't able to simulate the lows in atmospheric carbon dioxide found from proxies for the LGM. This is either due to not understanding the LGM mixing or not representing the oceans Carbon pumps accurately. These two issue should be investigated further. The oceans bio-chemical carbon cycle could be a cause of these lows. Another explanation could also be the abrupt change from PI to LGM forcing. In reality the glacial inter-glacial cycle is a smoother change. With in this changes to the carbon pumps and cover could the the cause for more carbon being removed from the atmosphere. Aswell as changes in the ocean mixing could be aving a similar effect. The SO windstress effect on the AMOC outflow and overturning need further investigation and its effects on the oceans carbon pump as the carbon pump could be the reason for the high CO_2 in the CESM LGM. The Model should also be investigated further using proxy reconstructions for salinity and precipitation. As well as doing investigation on how the model effect to an inter-glacial climate and various insolation forcings.

Acknowledgements

An Acknowledgment and thank you is due to the multiple organizations and people whose work and helped this thesis to be completed. A thanks to all the contributors to the CESM project and MARGO. A thanks is due to the Niels Bohr Institute based Team Ocean especially my supervisor Markus Jochum. Finally a thanks to all my friends and family who's support and encouragement helped me finish this thesis during a difficult time.

Bibliography

Brady, Esther C. et al. (2013). "Sensitivity to Glacial Forcing in the CCSM4". In: *Journal of Climate* 26.6, pp. 1901–1925. DOI: 10.1175/JCLI-D-11-00416.1. URL: https://journals.ametsoc.org/view/journals/clim/26/6/jcli-d-11-00416.1.xml.

Breitkreuz, Charlotte, André Paul and Michael Schulz (May 2019). "A dynamical reconstruction of the Last Glacial Maximum ocean state constrained by global oxygen isotope data". In: *Climate of the Past Discussions*, pp. 1–24. DOI: 10.5194/cp-2019-52.

Buckley, Martha W. and John Marshall (2016). "Observations, inferences, and mechanisms of the Atlantic Meridional Overturning Circulation: A review". In: *Reviews of Geophysics* 54.1, pp. 5–63. DOI: https://doi.org/10.1002/2015RG000493. eprint: https://agupubs.onlinelibrary.wiley.com/doi/pdf/10.1002/2015RG000493. URL: https://agupubs.onlinelibrary.wiley.com/doi/abs/10.1002/2015RG000493.

Clark, Peter U. et al. (2009). "The Last Glacial Maximum". In: *Science* 325.5941, pp. 710–714. DOI: 10.1126/science.1172873. URL: https://science.sciencemag.org/content/325/5941/710.

Gruber, Nicolas, Charles D. Keeling and Nicholas R. Bates (2002). "Interannual Variability in the North Atlantic Ocean Carbon Sink". In: *Science* 298.5602, pp. 2374–2378. ISSN: 0036-8075. DOI: 10.1126/science.1077077. eprint: https://science.sciencemag.org/content/298/5602/2374.full.pdf. URL: https://science.sciencemag.org/content/298/5602/2374.

Hays, J. D., John Imbrie and N. J. Shackleton (1976). "Variations in the Earth's Orbit: Pacemaker of the Ice Ages". In: *Science* 194.4270, pp. 1121–1132. DOI: 10.1126/science.194.4270.1121.

Hughes, Philip, Philip Gibbard and Jürgen Ehlers (Oct. 2013). "Timing of glaciation during the last glacial cycle: Evaluating the concept of a global 'Last Glacial Maximum' (LGM)". In: *Earth-Science Reviews* 125, pp. 171–198. DOI: 10.1016/j.earscirev.2013.07.003.

Jansen, E. et al. (2007). *2007: Palaeoclimate. In: Climate Change 2007: The Physical Science Basis. Contribution of Working Group I to the Fourth Assessment Report of the Intergovernmental Panel on Climate Change.*

Jochum, M. et al. (2010). "Response of air-sea carbon fluxes and climate to orbital forcing changes in the Community Climate System Model". In: *Paleoceanography* 25.3. DOI: https://doi.org/10.1029/2009PA001856. eprint: https://agupubs.onlinelibrary.wiley.com/doi/pdf/10.1029/

2009PA001856. URL: https://agupubs.onlinelibrary.wiley.com/doi/abs/10.1029/2009PA001856.

Jouzel, J., R.J. Suozzo R.D.Koster and G.L. Russell (1994). "Stable water isotope behavior during the last glacial maximum: A general circulation model analysis". In: *Journal of Geophysical Research: Atmospheres* 99.D12, pp. 25791–25801. DOI: https://doi.org/10.1029/94JD01819. eprint: https://agupubs.onlinelibrary.wiley.com/doi/pdf/10.1029/94JD01819. URL: https://agupubs.onlinelibrary.wiley.com/doi/abs/10.1029/94JD01819.

Kendall, C., J. J. McDonnell and Eric A. Caldwell (1998). *Isotope Tracers in Catchment Hydrology*. Chap. Fundamentals of Isotope Geochemistry.

Lang, C. et al. (1999). "16°C Rapid Temperature Variation in Central Greenland 70,000 Years Ago". In: *Science* 286.5441, pp. 934–937. DOI: 10.1126/science.286.5441.934.

Menary, Matthew B. et al. (2013). "Mechanisms of aerosol-forced AMOC variability in a state of the art climate model". In: *Journal of Geophysical Research: Oceans* 118.4, pp. 2087–2096. DOI: https://doi.org/10.1002/jgrc.20178. eprint: https://agupubs.onlinelibrary.wiley.com/doi/pdf/10.1002/jgrc.20178. URL: https://agupubs.onlinelibrary.wiley.com/doi/abs/10.1002/jgrc.20178.

Milankovitch, M. (1941). "Canon of Insolation and the Ice-Age Problem." In: *Israel Program for Scientific Translations*, p. 484.

Nielsen, S. et al. (2019). "Twotimescale carbon cycle response to an AMOC collapse". In: *Paleoceanography and Paleoclimatology* 34.4, pp. 511–523. DOI: https://doi.org/10.1029/2018PA003481.

Oberlander, E. Paul (n.d.). *REFINING THE MODEL, FOR A MORE RELIABLE FORECAST OF CLIMATE CHANGE*. URL: https://bit.ly/3cQEqv0. (accessed: 09.02.2021).

Sorooahian, Soroosf and Douglas G. Martinson (1995). *Natural Climate Variability on Decade-to-Century Time Scales, National Research Council*. Chap. PROXY INDICATORS OF CLIMATE. DOI: 10.17226/5142.

Stocker, Thomas F. and Sigfùs J. Johnsen (2003a). "A minimum thermodynamic model for the bipolar seesaw". In: *Paleoceanography* 18.4. DOI: https://doi.org/10.1029/2003PA000920. eprint: https://agupubs.onlinelibrary.wiley.com/doi/pdf/10.1029/2003PA000920. URL: https://agupubs.onlinelibrary.wiley.com/doi/abs/10.1029/2003PA000920.

— (2003b). "A minimum thermodynamic model for the bipolar seesaw". In: *Paleoceanography* 18.4. DOI: https://doi.org/10.1029/2003PA000920. eprint: https://agupubs.onlinelibrary.wiley.com/doi/pdf/10.1029/2003PA000920. URL: https://agupubs.onlinelibrary.wiley.com/doi/abs/10.1029/2003PA000920.

Talley, Lynne D. (Mar. 2013). "Closure of the Global Overturning Circulation Through the Indian, Pacific, and Southern Oceans: Schematics and Transports". In: *Oceanography*.

Zantopp, R. et al. (2017). "From interannual to decadal: 17 years of boundary current transports at the exit of the Labrador Sea". In: *Journal of Geophysical Research: Oceans* 122.3, pp. 1724–1748. DOI: https://doi.org/10.1002/2016JC012271. eprint: https://agupubs.onlinelibrary.wiley.com/doi/pdf/10.1002/2016JC012271. URL: https://agupubs.onlinelibrary.wiley.com/doi/abs/10.1002/2016JC012271.